

# Thermotropic liquid crystalline copolyesters with non-coplanar biphenylene units tailored for blend fiber processing with PET

Werner Grasser<sup>1</sup>, Hans-Werner Schmidt, Reiner Giesa\*

*Makromolekulare Chemie I, Bayreuth Institute for Macromolecular Research (BIMF) and Laboratory for Polymer Processing, Universität Bayreuth, D-95440 Bayreuth, Germany*

Received 3 March 2001; received in revised form 11 April 2001; accepted 20 May 2001

## Abstract

Via melt polycondensation two series of liquid crystalline thermotropic polyesters were synthesized for in situ reinforcement components in PET blend fibers. The copolymerization of a monomer bearing a bulky side group (*tert*-butyl hydroquinone) or a crankshaft monomer (6-acetoxy-2-naphthoic acid) with the non-coplanar 2,2'-dimethyl biphenol and terephthalic acid yielded two fully aromatic thermotropic polyesters. By varying and adjusting the individual monomer compositions, the melting behavior can be tailored to match the PET processing window. Solution viscosities up to  $\eta_{inh} = 6.57$  dl/g were achieved. By thermal characterization with DSC in combination with polarization microscopy up to 310°C neither a crystal melting point nor an isotropic transition was detected. Hence, the nematic polyesters solidify below the glass transition temperature into a glassy solid without crystallization. The polyesters are thermally stable above 400°C and form fluid melts. Fibers were spun from both series. Optimal processing was encountered at polyesters containing 60 mol% HNA, which could be spun continuously into high quality fibers. The fibers were characterized by tensile test, WAXS, and SEM. Fiber orientation was improved at a higher draw-down ratio and the Young's modulus was determined to 49 GPa at a tenacity of 550 MPa. © 2001 Elsevier Science Ltd. All rights reserved.

**Keywords:** Thermotropic copolyesters; *Tert*-butyl hydroquinone; Hydroxy naphthoic acid

## 1. Introduction

In the last decade several synthetic strategies for improving the solubility and lowering the melting transitions of thermotropic liquid crystalline polymers (TLCP) have been developed and are commonly employed in TLCP design. In general, this can be achieved by structural modification of the fully aromatic building blocks of the polymer chain without sacrificing the chain stiffness. Four important structural modifications are generally utilized and combined for the synthesis of processible, *para*-like aromatic TLCPs: (i) non-coplanar monomers, (ii) bulky side groups, (iii) the introduction of kinked, bent or crankshaft monomers, and (iv) the combination of all these structures in a copolymerization [1–3].

The structural modification (i) has proven to be especially effective in lowering transition temperatures while preserving maximum chain stiffness. 2,2'-substituted biphenols as non-coplanar units also maintain the rod-like nature of the

polyester backbone but the aromatic rings are forced out of plane by the substituents, thus twisting the unit [4–6]. Copolyesters containing this kind of monomers show dramatically decreased transition temperatures and enhanced solubilities compared to unsubstituted polymers. Melting temperature can also be reduced by using derivatives with bulky lateral substituents or flexible side chains [7–13]. With a combination of such structural modifications in copolymers, it is possible to suppress the crystallinity in TLCPs resulting in materials, which preserve the nematic order below the glass transition temperature and form nematic glassy solids [3,4,14].

Alternatively to lateral side groups, the polymer backbone can be modified with monomers introducing a crankshaft. These building blocks create a stepwise off-set in the polymer chain and therefore are also capable of reducing chain interactions without sacrificing backbone stiffness [1,6,9,10,15,16]. A typical crankshaft monomer is represented by 6-hydroxy-2-naphthoic acid (HNA), which is commercially employed in Vectra<sup>®</sup> type polyesters. Based on extensive research conducted by Jaffe and coworkers [17,18] on the spinning of Vectra<sup>®</sup>, TLCPs are spun routinely into fibers, and high-modulus engineering materials are obtained [19–21].

\* Corresponding author. Fax: +49-921-55-3670.

E-mail address: reiner.giesa@uni-bayreuth.de (R. Giesa).

<sup>1</sup> Mnemo science GmbH, 52074 Aachen, Germany.

TLCPs also have been studied extensively as possible reinforcing components in blends with thermoplastics, e.g. poly(ethylene terephthalate) (PET) [1,22–28], where the blends can be processed into highly oriented anisotropic morphologies leading to the formation of in situ composites possessing high strength and stiffness. The processing temperatures of PET blended with common TLCPs, such as the HBA/HNA copolyester series or Vectra<sup>®</sup>, typically needs to be increased to 300°C or higher. However, during melt processing it is crucial to keep temperatures sufficiently low to avoid thermal degradation and transesterification of PET [29–31].

The modulus of the blend fiber can be estimated from the blend concentration and intrinsic TLCP fiber modulus according to the rule of mixtures [28,35]. As a result, at higher concentrations the stiffening influence of the TLCP leads to a great loss in drawability of the PET blends. This disadvantage can be avoided through the use of block copolymers consisting of TLCPs and flexible blocks, which exhibit lower phase transitions and improved adhesion between the reinforcing and the matrix phase [23,26,32,33]. However, due to the flexible segments incorporated in the main chain this class of materials is likely to exhibit a low intrinsic fiber modulus. Thus, despite all these research efforts the need still exists for a tailored TLCP material that can be melt blended with PET to gain a considerable increase in mechanical performance compared to neat PET fiber.

The systematic investigation of the structure–property relationship in copolymer series of fully aromatic, rod-like TLCPs leading to nematic glasses is one objective of this contribution. It focuses on the development of TLCPs with the ability to (a) preserve the original drawing behavior of PET while (b) retaining the high fibril modulus of a fully rigid-rod structure. Furthermore, thermotropic copolyesters characterized by (c) high glass transition temperatures, (d) no crystallinity and a broad nematic phase and (e) sufficiently high molecular weights for fiber formation seem to be promising materials for the in situ reinforcement of PET blend fibers. To satisfy all these requirements with a single material is the challenge of this synthetic project. By varying the polyester structure, the melting range and melt viscosity of the polymers can be tailored for the desired processing conditions and thermoplastic matrix. The copolyesters described in this paper combine different aspects of chain interaction reduction: First the influence of a *tert*-butyl hydroquinone as comonomer in combination with a non-coplanar biphenol is studied. This bulky monomer has been used before in the successful synthesis of soluble and processible polyesters [34], but not as comonomer in this combination. Secondly, polyesters obtained by copolymerization of variable amounts of 6-hydroxy-2-naphthoic acid units as crankshaft comonomers in a fully aromatic backbone are investigated. The formation and properties of blends with PET and fibers spun thereof are published as the succeeding contribution in this journal [35].

## 2. Experimental

### 2.1. Materials

Terephthaloyl dichloride (**1b**) and 1-chloronaphthalene (Aldrich) were distilled at reduced pressure prior to use. Purified terephthalic acid (**1a**) was prepared by hydrolysis of terephthaloyl chloride (**1b**). *tert*-Butyl hydroquinone (**3**) (Fluka) was purified by sublimation. 6-Hydroxy-2-naphthoic acid (**5a**, HNA) was supplied by Hoechst Celanese Corporation. A 1:1 mixture by volume of trifluoroacetic acid (TFA) and chloroform was used for dissolving the polyesters. Other chemicals are commercially available and used as received.

#### 2.1.1. 4,4'-Dihydroxy-2,2'-dimethyl-biphenyl (**2a**)

**2a** was synthesized according to a literature procedure originally developed by Colon et al. [36] and modified by Percec et al. [37]. The oily raw material was distilled (160°C at 0.07 mbar) and recrystallized twice from toluene. The colorless crystals were dried in vacuo at 80°C for three days (yield: 50–60%, m.p. 154–156°C, Ref. [37]: 154–155°C). The <sup>1</sup>H NMR data were identical to values reported in Ref. [37]. <sup>13</sup>C NMR (DMSO-d<sub>6</sub>): δ (ppm) = 156.32 (C4), 136.96 (C1), 132.15 (C2), 130.74 (C6), 116.57 (C3), 112.73 (C5), 20.02 (CH<sub>3</sub>).

#### 2.1.2. 4,4'-Diacetoxy-2,2'-dimethyl-biphenyl (**2b**)

15 g (70 mmol) **2a** was stirred in 50 ml acetic anhydride containing some drops of conc. sulfuric acid for 2 h at 60°C. After cooling to RT the mixture was poured into 200 ml water, stirred for 1 h, extracted three times with ethyl ether, dried and distilled. The crude product was fractionated at 125–127°C and 0.1 mbar. The purified material solidified upon cooling (yield: 89%, m.p. 80–81°C). IR (KBr):  $\nu$  (cm<sup>-1</sup>) = 1760 (C=O). <sup>1</sup>H NMR (CDCl<sub>3</sub>): δ (ppm) = 7.33 (d, 2H, *meta* to CH<sub>3</sub> group), 6.96 (d, 2H, *ortho* to CH<sub>3</sub> group), 6.85 (dd, *para* to CH<sub>3</sub>), 2.35 (s, 6H, O(CO)CH<sub>3</sub>), 2.26 (s, 6H, CH<sub>3</sub>).

#### 2.1.3. Acetoxy-2-naphthoic acid (**5b**)

6-Hydroxy-2-naphthoic acid (**5a**) (25 g, 0.181 mol) and 150 ml acetic anhydride were refluxed at 150°C for 8 h. After removal of excess acetic anhydride by distillation the crude product was dried at 80°C in vacuo for 5 h and recrystallized from chloroform (yield: 90%, m.p. 222–223°C). IR (KBr):  $\nu$  (cm<sup>-1</sup>) = 1762 (C=O). <sup>1</sup>H NMR (CDCl<sub>3</sub>): δ (ppm) = 13.1 (s, 1H, COOH), 8.65 (s, 1H, H1), 8.17 (d, 1H, H4), 8.0 (m, 2H, H3 and H8), 7.76 (d, 1H, H5), 7.42 (dd, 1H, H7), 2.35 (s, 3H, O(CO)CH<sub>3</sub>).

### 2.2. Polymer synthesis

All polyesters (see Table 1) were synthesized via melt polycondensation in a one-step procedure. Copolyesters **4** were obtained by reacting terephthaloyl dichloride (**1**),

Table 1

Synthetic methods, solubility behavior, inherent viscosities, and thermal properties of copolyesters **4** and **6**. (–) insoluble, (o) partially soluble at elevated temperatures, (+) soluble upon heating, (+ +) soluble at room temperature

Polymer	$x$	$T_{\text{synth}}/t_{\text{react.}}$ (°C)/(h)	Solubility in		$\eta_{\text{inh}}^a$ (dl/g)	$T_g^b$ (°C)	$T_{-5\%}^c$ (°C)	$T_{-10\%}$ (°C)
			CHCl <sub>3</sub>	TFA/CHCl <sub>3</sub>				
<b>4a</b>	0.4	280/7.5	o	++	1.30	142	440	465
<b>4b-1<sup>d</sup></b>	0.5	280/7.5	++	++	1.14	144	420	458
<b>4b-2</b>	0.5	280/8.5 st <sup>e</sup>	+	++	4.61	166	436	455
<b>4b-3</b>	0.5	280/8.5 st	+	++	5.32	168	444	465
<b>4b-4</b>	0.5	280/8.5 st	+	++	5.55	166	451	470
<b>4b-5</b>	0.5	280/8.5 st	o	++	6.57	171	454	469
<b>4b-6</b>	0.5	280/8.5 <sup>f</sup> st	++	++	1.55	149	431	462
<b>4c</b>	0.6	280/7.5	+	++	1.33	154	463	480
<b>4d</b>	0.7	280/7.5	o	++	1.43	157	449	459
<b>6a</b>	0	280/7	–	++	1.04	n/a	414	438
<b>6b</b>	0.2	280/7	–	++	0.54	97	415	440
<b>6c</b>	0.3	280/7	–	++	1.09	99	455	471
<b>6d</b>	0.45	280/7	–	++	1.63	101	465	476
<b>6e-1</b>	0.6	280/7	–	++	2.05	98	476	486
<b>6e-2</b>	0.6	280/10	–	++	2.09	103	458	487
<b>6e-3</b>	0.6	280/7 <sup>g</sup>	–	++	2.52	105	476	485
<b>6e-4</b>	0.6	300/6 <sup>g</sup>	–	++	3.41	113	470	482
<b>6e-5</b>	0.6	300/7 <sup>g</sup>	–	++	3.86	108	483	492
<b>6f</b>	0.7	280/7	–	o	–	94	390	466
<b>6g</b>	0.8	280/7	–	–	–	111	475	488

<sup>a</sup> Determined in TFA/CHCl<sub>3</sub> = 1 : 1 (v/v) at 25°C,  $c = 0.2$  g/dl.

<sup>b</sup> N<sub>2</sub>, 10 K/min, 2nd heating cycle.

<sup>c</sup> N<sub>2</sub>, 10 K/min.

<sup>d</sup> Same composition, different experiments are indicated by a run number.

<sup>e</sup> Stainless steel spiral stirrer, see text for more details.

<sup>f</sup> Molecular weight regulated by the addition of 4.5 mol% of hydroquinone monomethylether.

<sup>g</sup> With purified terephthalic acid.

4,4'-dihydroxy-2,2'-dimethyl-biphenyl (**2**) and *tert*-butyl hydroquinone (**3**) without a base according to Scheme 1. The reaction was performed in a glass reactor equipped with a glass stirrer and an inert gas inlet. To obtain higher molecular weights a spiral-shaped stainless steel stirrer was used instead of a simple glass stirrer for highly viscous melts. For example, the synthesis of polyester **4b** ( $x = 0.5$ ) is described: a monomer mixture of 1.137 g (5.6 mmol) **1**, 0.600 g (2.8 mmol) **2** and 0.465 g (2.8 mmol) **3** was placed in a glass reactor under a constant argon flow, and held for 1 h at 100, 110, and 120°C, respectively. Over a period of 2 h the melt was heated to 270°C and stirred at this temperature for 1 h before vacuum was applied for 2.5 h to complete the reaction. The solidified polyester was dissolved in TFA/chloroform and precipitated twice from methanol. The product was extracted with isopropanol for 48 h and dried in vacuo.

For polyesters **6** the synthetic procedure was modified. Terephthalic acid (**1**), 4,4'-diacetoxy-2,2'-dimethyl-biphenyl (**2**) and 6-acetoxy-2-naphthoic acid (**3**) were polycondensated without a catalyst (see Scheme 1). Since the polyesters formed fluid melts, all reactions were stirred with a glass stirrer. For example, the synthesis of polyester **6e** ( $x = 0.6$ ) is described. A monomer mixture of 1.661 g

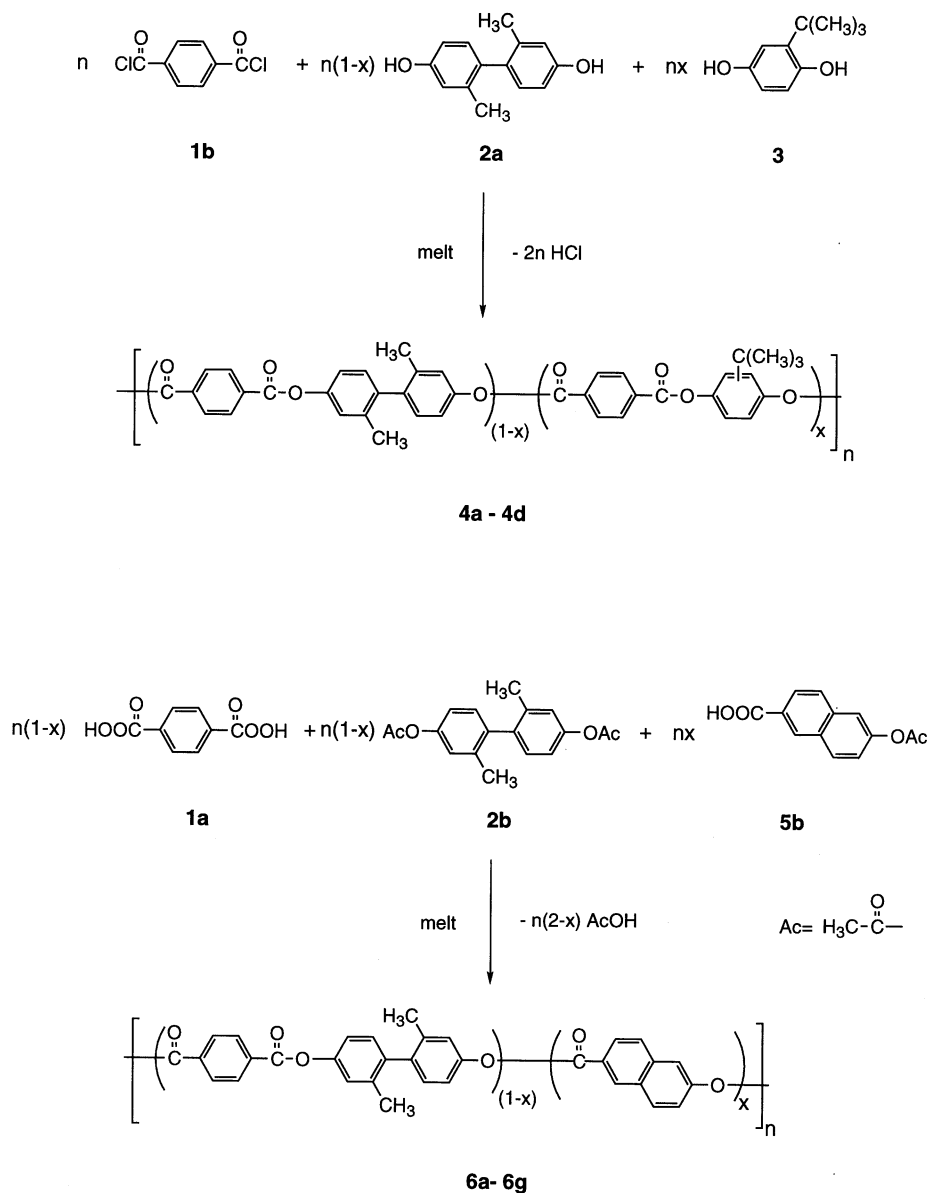
(10 mmol) **1**, 2.983 g (10 mmol) **2** and 3.453 g (15 mmol) **3** was placed in a glass reactor, heated to 200°C over 1 h and to 280–300°C during an additional hour while the acetic acid formed was removed by a continuous argon flow. The melt was stirred at this temperature for 1 h prior the application of vacuum for 4 h to complete the reaction. The polyesters were removed from the reactor and used without further purification. Synthetic variations for different copolyesters compositions are also included in Table 1.

### 2.3. Fiber processing

Polyesters were spun at 265–290°C using a capillary melt spinner (RheoMeltfixer, SWO, Germany) equipped with a conical-shaped die (bore diameter: 500 μm). The plunger speed was carefully increased until a continuous strand was extruded. The material was first stretched slightly by hand and, if no breakage occurred, drawn and taken-up on commercial fiber spools by a motor with adjustable speed.

### 2.4. Characterization

Differential scanning calorimetry (DSC) was carried out with a Perkin-Elmer DSC7 system in the range of 20–310°C at heating and cooling rates of 10 K/min. The instrument was calibrated with indium regarding temperature and enthalpy.



Scheme 1.

Thermogravimetric analysis (TGA) was performed on a Netzsch STA 409 in the temperature range of 20–650°C at a heating rate of 10 K/min and a nitrogen flow rate of 75 ml/min. Melt rheology was analyzed on a Rheometric Scientific Stress Rheometer SR 5000 under nitrogen. Solution viscosities were determined at concentration of 0.2 g/dl with a Schott–Ubbelohde viscometer (capillary type: 0a) at 25°C in TFA/chloroform. GPC measurements were performed on a Waters model 590 equipped with UV- and RI-detectors. The eluent was chloroform (1 ml/min) and standard polystyrene calibration was used for calculating molecular weights. <sup>1</sup>H NMR spectra were recorded on a Bruker A 250 at 250 MHz in chloroform-d<sub>3</sub> at RT. Liquid crystalline textures were investigated on a Leitz Laborlux 12-pol optical polarization microscope equipped with a Mettler FP-82 hot-stage. Tensile tests were performed

on an Instron Universal Tester (Floor Model 5565, 5kN Frame) with a 100 N load cell and 100 N pneumatic grips with rubber jaw faces. Fibers were tested at room temperature according to ASTM Method D3379 using a gauge length of 50 mm and 0.2 mm/min crosshead speed. Based on this method, monofilaments were mounted on paper tabs to improve fiber handling. Prior to testing the diameter of the monofilaments were determined with an optical microscope (Olympus BX60) at a magnification of 1000 after calibration with a Leitz dimensional standard. Scanning electron microscopy (SEM) investigations were carried out on a Jeol JSM 840 A at 10–20 keV. For sample preparation, the fibers were cryofractured in liquid nitrogen and sputtered with gold. Wide angle X-ray diffraction pattern were obtained on a Seifert Isoflex 3000 (Cu K<sub>α</sub>

at 2.5 kW) equipped with a fiber set-up in a Laue camera.

### 3. Results and discussion

#### 3.1. Synthesis

The development of melt processible, fully aromatic, high molecular weight, thermotropic polyesters in form of nematic glasses as in situ reinforcement components in PET blend fibers is the objective of this work. Several structural concepts were employed to meet these demands: (i) non-coplanar monomers such as 2,2'-disubstituted biphenyls introduce a strong twist in the backbone, which is caused by the repulsive interactions of the methyl substituents; (ii) lateral bulky substituents induce positional isomerism along the backbone and prevent close chain packing and thus crystallization, (iii) the introduction of a crankshaft monomer in the polymer backbone induces a stepwise offset while preserving chain rigidity; (iv) A–B type monomers introduce statistical variations into the chain and therefore lower the inter-chain interactions and (v) the incorporation of all these structures in a copolyester, to interrupt the inter-molecular interaction by random placement the monomers. Copolyesters with good mechanical performance are characterized by a decent molecular weight, which is in return only accessible by melt polycondensation. Two series of copolyester were synthesized; series **4** with *tert*-butylhydroquinone as a monomer with a bulky side chain and series **6** with HNA as a typical crankshaft monomer. The polyester synthesis is outlined in Scheme 1.

Biphenyl **2a** was synthesized based on a reductive coupling procedure starting with 4-chloro-3-methylphenol [36,37]. The product does not crystallize and is obtained as an oily liquid. Distillation yields a glassy solid, which can be purified by recrystallization from toluene.

Terephthaloyl dichloride (**1b**), 4,4'-dihydroxy-2,2'-dimethyl-biphenyl (**2a**) and *tert*-butyl hydroquinone (**3**) were used to synthesize copolyester **4a–d** with compositions between 40 and 70 mol% of **3**. Other compositions were realized via solution polycondensation yielding insoluble and intractable low molecular weight materials [38]. For copolyesters **6**, acetylated monomers were employed, which can be easily purified and are not water sensitive, thus are the best choice for A–B monomers such as HNA, since the corresponding acid chloride is difficult to synthesize and handle. Copolyesters **6a–g** were synthesized according to Scheme 1 by melt polycondensation of terephthalic acid (**1a**), 4,4'-diacetoxy-2,2'-dimethyl-biphenyl (**2b**) and 6-acetoxy-2-naphthoic acid (**5b**) with copolymer compositions up to 80% of **5b**. The individual compositions, polycondensation runs and data, which are discussed later are listed in Table 1.

To optimize molecular weight, different synthetic conditions and runs at the same copolyester composition were

tested, which are indicated in Table 1 by a run number. Inherent viscosities of polyesters with the same comonomer composition permit a direct comparison of their molecular weight. A spiral-shaped stainless steel stirrer, which enables mixing even at high melt viscosities, can provide better mixing. For **4b** the molecular weight was greatly improved by this technique and inherent viscosities up to 6.57 dl/g (**4b-5**) were achieved. Series **6** exhibited greatly reduced melt viscosities and a standard glass stirrer furnished sufficient agitation. The most noticeable influence for **6e** was caused by an increase of the final reaction temperature from 280 to 300°C. Careful purification of terephthalic acid via hydrolysis of the acid dichloride was another method to increase molecular weight (see Table 1, **6e-3**, **-4** and **-5**). Longer reaction times under vacuum revealed a small influence on molecular weight. Under optimized conditions polyesters with inherent viscosities up to 3.8 dl/g (**6e-5**) could be synthesized. However, in particular for in situ composites, the melt viscosity of the reinforcing compound must be in a certain relationship with the melt viscosity of the matrix [35,39]. Therefore a control of the molecular weight is desired and was tested by employing a monofunctional end-capping agent for polyester **4b-6**, which resulted in a decreased viscosity of 1.55 dl/g.

#### 3.2. Solubility tests

All polyesters of series **4** are completely soluble in solvents for aromatic polycondensates, such as *p*-chlorophenol, a mixture of trifluoroacetic acid (TFA)/chloroform, selected polyesters also in chloroform. The best solubilities were found at a comonomer feed of **4b** at 50 mol%.

In comparison, copolyesters **6** are insoluble in common organic solvents such as chloroform or THF, even at elevated temperatures. The polycondensates are soluble only in special solvents, such as *p*-chlorophenol or preferably at room temperature in a mixture of equal volumes of TFA and chloroform. In this mixture, polyesters **6a–e** are completely soluble at room temperature, while polymer **6f** ( $x = 0.7$ ) is only partially soluble, and **6g** ( $x = 0.8$ ) is completely insoluble at this temperature (see Table 1). This observation can be explained by a higher HNA content, which induces a progressing stiffening of the polymer chain. Polyester **6e** was synthesized with different molecular weights, where the solubility of the polymers remained almost unaffected by the molecular weight but dissolving times were found to be longer.

For all polyesters inherent viscosities were measured in TFA/chloroform (1:1/v:v) at 25°C at a concentration of 0.2 g/dl. The viscosities ranged between 1.04 and 6.57 dl/g and all data are listed in Table 1. It is evident that stirring of the reaction mixture, especially at higher melt viscosities is important for achieving higher molecular weights. Viscosity values for series **6** ( $\eta_{inh} = 3.86$  dl/g) with HNA are lower compared to the highest viscosities measured for series **4** ( $\eta_{inh} = 6.57$  dl/g) with *tert*-butyl hydroquinone.

Even after considering differences in molecular weight, we believe that this reflects a clear decrease in chain stiffness introduced by HNA compared to *tert*-butyl hydroquinone.

### 3.3. Size exclusion chromatography (SEC) and NMR spectroscopy

Copolyesters **6** are insoluble in common organic solvents such as chloroform or THF, even at higher temperatures, thus no characterization with size exclusion chromatography (SEC) or NMR was possible with the equipment available.

For series **4** SEC measurements were performed with polymers completely soluble in chloroform at room temperature and at polymer concentrations of 0.5 g/dl. Values for  $M_n$  and  $M_w$  were determined with a polystyrene standard calibration. In particular for rigid polymers, including the TLCPs presented here, a polystyrene calibration will generally produce incorrect absolute molecular weight data. Therefore all molar masses are relative values and can be compared to each other only. All results are included in Table 2. Polyester **4b-1** and **4b-4** are identical in chemical composition but were synthesized using a glass stirrer or a stainless steel spiral stirrer, respectively.  $M_w$  and  $M_n$  show the same dependence on the synthetic method as already observed for inherent viscosities. Values between 6000 and 11,000 g/mol are calculated. For mixtures additionally agitated at high viscosities with a stainless steel stirrer,  $M_n$  is above 40,000 g/mol. The molecular weight distributions are monomodal with broad polydispersities around 4–5 for  $M_w/M_n$ .

The proton-NMR spectra in deuterated chloroform show signals typical for the incorporated monomers. The *tert*-butyl group of **3** has a characteristic signal between 1.3 and 1.5 ppm, methyl groups of **2a** are responsible for a signal between 2.0 and 2.3 ppm. The chemical shifts of the aromatic protons of the diol components are found in the range of 6.5–7.5 ppm while terephthalic acid exhibits resonance between 8.0 and 8.5 ppm.

The characteristic signals of the methyl group and the *tert*-butyl groups enable the determination of copolymer compositions. The results are compared in Table 2 and

Table 2  
Calculated and experimental copolymer compositions, inherent viscosities, molecular weight and polydispersity by SEC of selected copolyesters **4**

Polymer	$x_{\text{theor}}$	$x_{\text{NMR}}^a$	$\eta_{\text{inh}}^b$ (dl/g)	$M_n^c$ (g/mol)	$M_w^c$ (g/mol)	$M_w/M_n$
<b>4a</b>	0.4	0.40	1.30	10200	39800	3.92
<b>4b-1</b>	0.5	0.51	1.14	6800	36300	5.38
<b>4b-4</b>	0.5	0.50	5.55	41300	185400	4.49
<b>4c</b>	0.6	0.62	1.33	11000	51300	4.68
<b>4d</b>	0.7	0.70	1.43	10900	56700	5.22

<sup>a</sup> <sup>1</sup>H NMR in chloroform- $d_3$  at RT.

<sup>b</sup> In TFA/chloroform (1:1/v:v) at 25°C,  $c = 0.2$  g/dl.

<sup>c</sup> In chloroform, standard polystyrene calibration.

experimental values are in good agreement with the comonomer feed.

### 3.4. Thermal properties

All polyesters were characterized regarding their thermal stability with TGA and possible phase transitions with DSC. The results are also included in Table 1. To indicate the thermal stability of the polymers, the temperatures corresponding to 5 and 10% weight loss are listed. The thermal stability of the materials is excellent to 400°C and above in a nitrogen atmosphere. The inferior thermal stability of the *tert*-butyl group, which is reported to degrade into isobutene at higher temperatures [34] is not evident for the higher molecular weight polyesters of series **4** presented here, however, was observed for lower viscosity solution polycondensates [38].

DSC measurements of the copolyesters did not reveal any thermal transitions between 20 and 310°C other than glass transitions. The glass temperatures ( $T_g$ ) of series **4** were determined to range between 142 and 171 °C, therefore clearly higher than those of series **6** ranging between 94 and 113 °C, this decrease being associated with a lower chain stiffness induced by the HNA crankshaft. No endothermic melting peaks could be detected up to 310°C, thus the samples are considered completely amorphous in this temperature range. The  $T_g$  does not show any obvious dependence on the copolymer composition. The differences mainly have to be attributed to the variations in molecular weight. Especially at low molecular weight, the glass transition temperature is strongly dependent on the chain length, since the contribution of chain ends to the free volume of the polymer is larger than for segments within the chain. Therefore glass transition temperatures level off at higher molecular weights, which has been shown for polymers in general [40] and also in particular for TLCPs [1]. This effect can be demonstrated for polyesters **4b** and **6e**, since different molecular weights but structurally identical polymers, have been synthesized in the course of this work. Plotting the glass temperatures versus the corresponding inherent viscosity, as shown in Fig. 1, illustrates the dependence of the glass temperature on the molecular weight of the liquid crystalline polyesters.

The melting behavior of the copolyesters was tested preliminarily on a high-temperature hot stage. For series **4** liquid crystalline melts are obtained below 300°C. Melt viscosities were tested qualitatively by simple shear tests and are clearly higher for high molecular weight samples. Polyesters **4a–4d** soften slowly when heated above their glass transition temperatures and noticeable deformation is possible at ca. 200°C. Softening behavior depends on the comonomer composition and was found to be optimal for copolyester **4b** ( $x = 0.5$ ).

For series **6** a clear dependence of the  $T_g$  on the amount of HNA incorporated in the copolyester can be established. Homopolymer **6a** and copolymer **6g** ( $x = 0.8$ ) do not soften

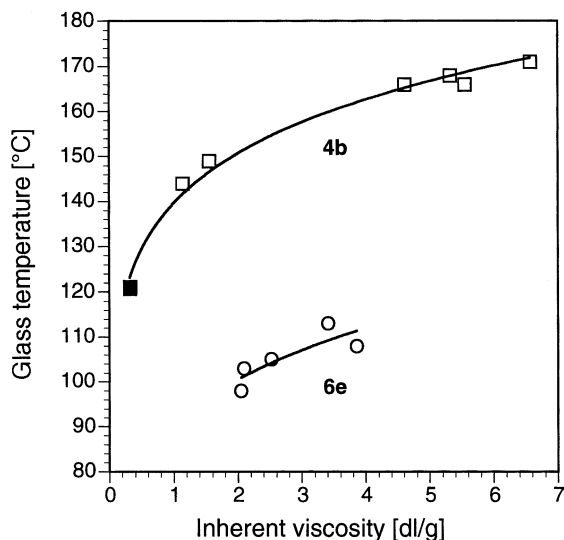


Fig. 1. Glass transition temperature as function of the inherent viscosity of polyesters **4b** (open squares) and **6e** (open circles). (First value for **4b** (■) was taken from Ref. [38]).

below 300°C. Polyesters **6b–6f** soften slowly when heated above their  $T_g$  and noticeable deformation is possible at ca. 150°C. At 280°C they are fluid melts, which exhibit opalescence upon shearing (vide infra). Thus incorporation of HNA produces a significant drop of the softening temperature. For polyester **6e-2** the melt viscosity as a function of the temperature was determined with a stress-strain rheometer in a plate–plate geometry. The melt viscosity decreases continuously when the polymer is heated above  $T_g$  under oscillating shear conditions. This is illustrated in Fig. 2 where the zero-shear viscosity of **6e-2** is plotted versus the temperature up to 300°C. In contrast, the viscosity of semi-crystalline LC polyesters decreases by several orders of magnitude around the crystal melting temperature within a range of 20–30°C [41]. In the present case softening takes place slowly over a broad temperature range since the melt is not filled with crystallites due to the completely amorphous character of the material.

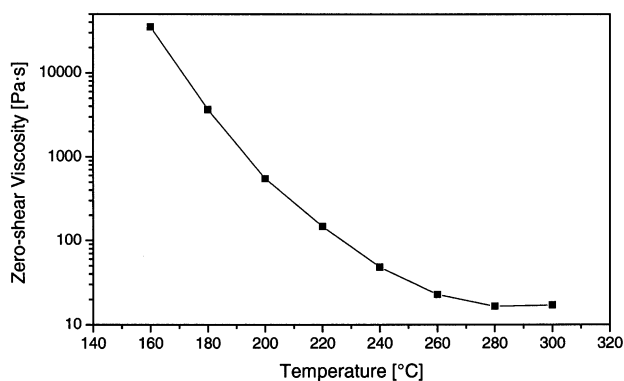


Fig. 2. Temperature dependence of the zero-shear viscosity for polyester **6e-2**.

### 3.5. Polarized optical microscopy

All polyesters soften slowly at 30–50°C above their glass transition temperatures. No transition into an isotropic phase is detectable below 310°C. The absence of crystallinity in the copolyesters is also indicated by the lack of transitions between crystalline and liquid crystalline phases. Upon cooling below  $T_g$  the nematic phases of polymers **4** and **6** are frozen in a glassy state. The formation of nematic glasses is independent of the cooling rate and no crystallization was observed even after annealing for days. A clear identification of a nematic texture is only possible for lower molecular weight samples since these are capable of forming typical marbled features, which are shown for **6e-1** in Fig. 3a and are often observed for nematic liquid crystals [6]. In some cases threaded textures could be observed at higher temperatures, which were preserved after cooling to room temperature (see Fig. 3b and c). Higher molecular weight polyesters form birefringent melts but the formation of a typical nematic texture is hindered by high melt

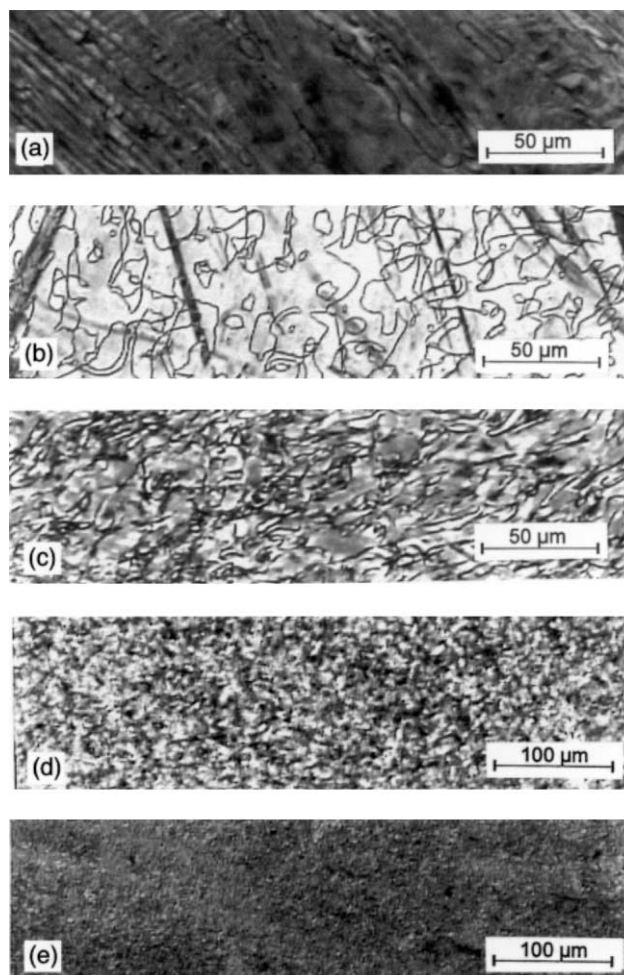


Fig. 3. Optical polarized micrographs of polyester, (a) **6e-1**, at 250°C (b) **6e-1**, at 280°C (c) **6e-1**, after cooling to room temperature (d) **6e-5**, at 300°C (e) **4b-3**, the sample was heated first to 300°C, then cooled to 280°C, where the depicted texture was observed.

Table 3

Young's modulus ( $E$ ), strength ( $\sigma_{\max}$ ) and elongation at break ( $\epsilon_{\max}$ ) of **4b** and **6e** fibers as function of the die temperature and take-up speed (standard deviation given in parenthesis). n/c: no continuous spinning possible

Entry	Polymer	$\eta_{\text{inh}}$ (dl/g)	$v^a$ (m/min)	$T_{\text{die}}$ (°C)	$D^b$ ( $\mu\text{m}$ )	$E$ (Gpa)	$\sigma_{\max}$ (Mpa)	$\epsilon_{\max}$ (%)
1	<b>4b-3</b>	5.32	n/c	280	167 (30)	15.75 (3.55)	261 (83)	7.68 (3.82)
2	<b>4b-3</b>	5.32	n/c	290	85 (16)	20.97 (5.84)	289 (89)	2.99 (1.30)
3	<b>6e-2</b>	2.09	44	260	48 (6)	41.36 (6.67)	269 (50)	0.71 (0.07)
4	<b>6e-2</b>	2.09	70	265	45 (5)	42.41 (4.29)	244 (46)	0.64 (0.14)
5	<b>6e-2</b>	2.09	120	265	28 (5)	45.61 (3.42)	243 (55)	0.55 (0.13)
6	<b>6e-5</b>	3.86	30	270	86 (11)	46.71 (2.15)	529 (43)	1.36 (0.15)
7	<b>6e-5</b>	3.86	80	270	77 (9)	48.64 (1.87)	548 (28)	1.34 (0.12)
8	<b>6e-5</b>	3.86	100	270	81 (9)	47.81 (2.56)	480 (80)	1.15 (0.21)

<sup>a</sup> Take-up speed.

<sup>b</sup> Fiber diameter.

viscosities. The small granular domain structure of these melts impedes a clear identification of the liquid crystalline phase. This type of texture is depicted in Fig. 3d for **6e-5**. For the same reason the identification of the liquid crystalline phase is also difficult for polyesters **4b**, **c**, and **d**. The polymer melts are birefringent and show a small granular domain structure upon heating to 300°C as shown in Fig. 3e for **4b-3**.

### 3.6. Fiber formation and properties

#### 3.6.1. Fiber spinning

During preliminary experiments on a hot-stage polyesters **4b** revealed relatively low melt viscosities and therefore were chosen for fiber spinning experiments. The materials were extruded with a constant piston speed of 0.6 mm/min through a conical die attached to a capillary melt spinner. Extrusion of **4b-3** into strands was successfully performed at 280°C. However, as soon as the strand was slightly drawn by hand or a fiber take-up device, breakage occurred. Raising the die temperature to 290°C resulted in a slightly better performance but the weakness of the polymer melt towards drawing prevented a continuous drawing process and thus the formation of a homogeneous fiber. The obtained strands were brittle and did not show any fibrous morphologies typical for LCP-fibers [17,18] indicating weak orientation in the polyester fiber. Higher processing temperatures sometimes cause side reactions, in addition could not be tested due to a lack of material. In conclusion, the melt of polyester **4b** can be extruded but the viscosity is still too high to obtain good fibers.

For polyesters **6b–f** short strands could be drawn by hand on a hot-stage at 280°C. The resulting strands or fibers are short and brittle at low HNA contents. However, fiber formation is improved for higher HNA levels and longer fibers were obtained easily for polyester **6e** ( $x = 0.6$ ). Further increase in the HNA content again was accompanied by higher brittleness. Based on these preliminary experiments, polymer **6e** was considered most suitable for fiber spinning experiments in this series. Thus polyesters **6e-2** and **-5** with inherent viscosities of 2.09 and 3.86 dl/g,

respectively, were employed for fiber spinning. Optimal processing conditions were found at die temperatures between 260 and 270°C. Higher temperatures resulted in very low melt viscosities so that continuous spinning process was impossible. Lower temperatures are below the processing window for PET and furthermore led to frequent breakage during spinning. Take-up speeds of up to 120 m/min were achieved for both samples. At higher speeds, the fiber diameter decreases dramatically and therefore frequent failure occurred during spinning. The stretch ratio is determined as the ratio between the bore diameter (500  $\mu\text{m}$ ) and the stretched fiber cross-sections. In preliminary experiments the fibers exhibited good mechanical performance along the fiber axis but easily break upon bending and a fibrous, woodlike fracture surface (vide infra) typical for TLCPs [17,18] could be observed.

#### 3.6.2. Fiber testing

Despite frequent breakage during fiber spinning of **4b-3**, short fiber strands were investigated in a tensile test. Mechanical data, such as Young's modulus, strength and elongation at break were determined for fibers extruded at die temperatures of 280 and 290°C. The results are included in Table 3 as entries 1 and 2. The die temperature has a significant influence on the mechanical performance of the fibers. Raising the temperature resulted in fibers with half the diameter indicating an improved down-draw. Young's modulus is increased from 16 to 21 GPa. Ultimate elongation decreases from 7.7 to 3.0 % while fiber tenacity remains constant. Nevertheless, the overall mechanical performance of the fibers is disappointing compared to other TLCP fibers.

In contrast, fibers of good quality of polyesters **6e-2** and **-5** were obtained continuously at different take-up speeds. Mechanical data were evaluated as function of take-up speed during fiber spinning, molecular weight of the polymers and die temperature. All mechanical data are listed in Table 3, and a graphic representation of data is displayed in Fig. 4. Young's moduli of the fibers attained 40 and 50 GPa and reveal only little variation with molecular weight. The moduli of fibers of **6e-2** ( $\eta_{\text{inh}} = 2.09$  dl/g, entries 3–5) slightly increase with increasing take-up speed indicating



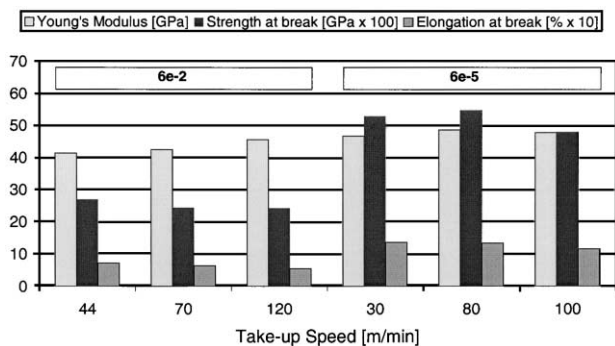


Fig. 4. Graphical presentation of the mechanical performance as function of the take-up speed for **6e-2** and **6e-5** fibers.

a better orientation at higher speeds, which was also confirmed by wide-angle X-ray diffraction (WAXS) measurements, which are discussed later. Higher molecular weight sample **6e-5** ( $\eta_{inh} = 3.86$  dl/g, entries 6–8) does not show this effect and the moduli are barely affected by the stretch ratio. Obviously, the elongational flow present during extrusion spinning is not capable of producing better orientation in the fibers at higher molecular weights. However, an increase in molecular weight has a more distinguished effect on strength and elongation at break. The higher molecular weight sample **6e-5** exhibits twice the values compared to **6e-2**. This effect of the increasing molecular weight on mechanical properties has been also observed for other TLCP fibers [42]. Overall mechanical performance of the LCP fibers is comparable to fibers spun from other glassy nematic polyesters [14] and greatly improved compared to series **4**.

### 3.6.3. Fiber morphology

Fiber fracture surfaces obtained by breaking the fibers in liquid nitrogen were investigated with SEM. A microstructure is present for a fiber spun from **4b** (Fig. 5a) but much less pronounced than those visible for **6e** (Fig. 5b and c) or in other TLCP fibers. In some regions ribbon-like substructures are visible oriented along the fiber axis. High melt viscosity prevents orientation during spinning. In contrast, lower melt viscosity allows higher stretch ratios and therefore better orientation of the polymer chains. Since mechanical performance often is related to the extent of fibrillation [17,18,43] this is a plausible reason for the poor mechanical behavior of **4b** fibers. A skin-core morphology, which has been observed for other TLCP fibers and extrudates [44,45] is not present.

For fibers spun from copolyester **6e** SEM investigations reveal a woodlike, hierarchic structure, which is depicted in Fig. 5b and c for fiber spun at 265 °C (entry 5). Here a typical fibrillar microstructure of the LCP fibers is evident. The fibers consist of bundles 0.5–1  $\mu\text{m}$  in diameter. Orientation of the material increases from the core to the skin region of the fiber. The core has a more blocky substructure while the outer regions are dominated by a fibrillar structure

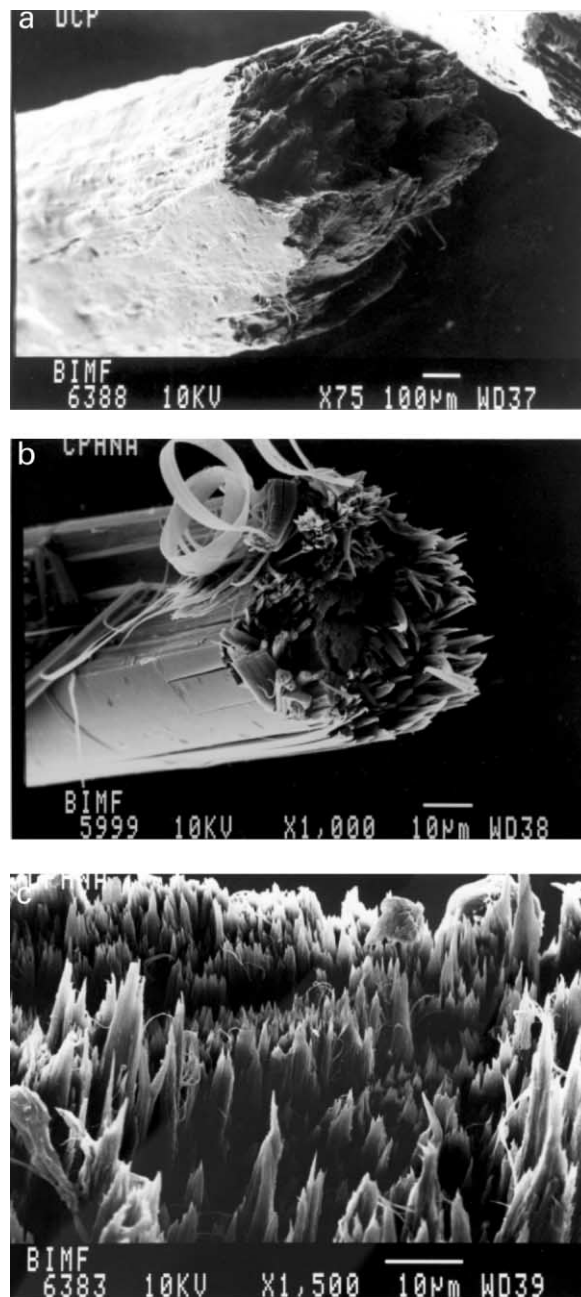


Fig. 5. SEM cross-sections of fracture surfaces of selected copolyester fibers: (Entries refer to Table 3). (a) **4b-3**, entry 2: total view (b) **6e-2**, entry 5: total view (c) **6e-2**, entry 5: detailed view.

(Fig. 5c). In most cases ribbon-like structures can be found, which again consist of smaller sized fibrils. As documented in the literature, mechanical performance of the fibers is related to the extent of fibrillation and the length of the fibrils sticking out of the cross-section [17,18,43]. A skin-core morphology typical for TLCP fibers and extrudates [44–46] is also recognizable in the thin and highly oriented outer regions of the polyester fibers (Fig. 5b). Thus the fiber morphological studies confirm the differences observed in mechanical performance of the fiber spun from **4b** and **6e**.

Table 4  
X-ray diffraction data of fibers spun from **6e-2** presented as  $2\theta$ -reflection angles and the corresponding  $d$ -spacing (at Cu  $K\alpha$ -radiation)

Position	$2\theta$ (°)	$d$ (nm)
Equatorial	9.6	0.92
	17.4	0.51
Meridional	12.0	0.74
	22.1	0.40
	39.5	0.23
	43.9	0.21

### 3.7. Wide-angle X-ray diffraction

To investigate LCP orientation and detect crystallinity in the fibers, WAXS patterns of fibers spun from **6e-2** were recorded using a Laue fiber camera set-up. The diffraction patterns exhibit two sets of equatorial and four sets of meridional reflexes and their  $2\theta$  positions and corresponding  $d$ -

spacing are listed in Table 4. In Fig. 6 two sets of diffraction patterns are depicted. Fig. 6a shows the pattern obtained for fibers processed at low take-up speeds (70 m/min, entry 4), whereas the pattern in Fig. 6c corresponds to fibers spun at 120 m/min (entry 5). To clearly distinguish the meridional reflexes an overexposed pattern is shown additionally in each set (Fig. 6b and d). The existence of two Bragg maxima at the equator indicates a two-dimensional order of the polymer chains. The meridional reflexes represent the distribution of the monomer units along the chain [47]. Aperiodic maxima, like in the present case, indicate a statistical copolymer [10]. The amorphous character of polymer **6e-2** is demonstrated by the absence of reflexes off the equator or meridian, since a three-dimensional order within the fiber is indicated by sharp off-equatorial reflexes [48].

As shown in Fig. 6a and c fibers spun from **6e-2** ( $\eta_{inh} = 2.09$  dl/g) show sharper reflexes with increasing take-up speed indicating an improved orientation. This corresponds to the observed increase in Young's modulus (Table 3).

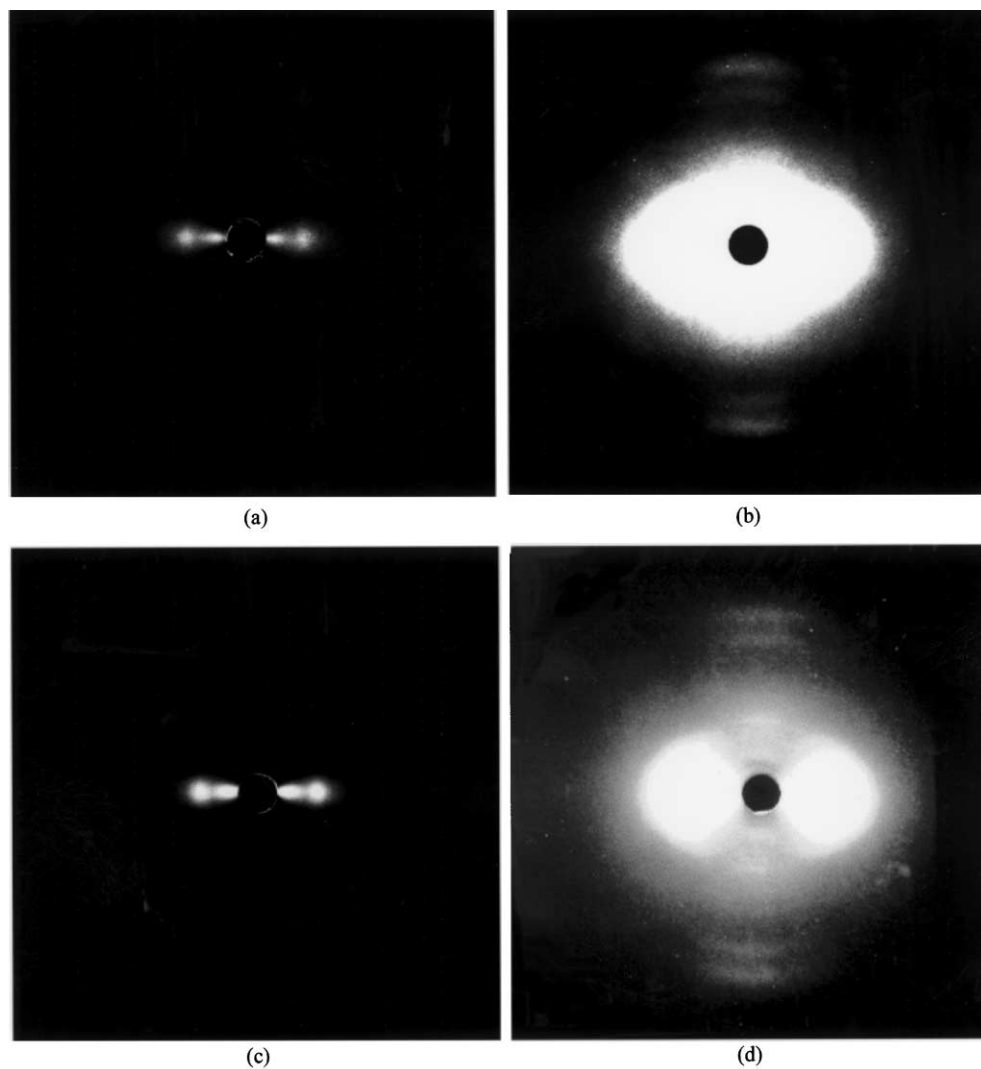


Fig. 6. Wide-angle X-ray diffraction patterns of fibers from **6e-2** (fiber axis is vertical, entries refer to Table 3). (a) take-up speed 70 m/min (entry 4) (b) same as (a), with overexposed equatorial reflexes (c) take-up speed 120 m/min (entry 5) (d) same as (c) with overexposed equatorial reflexes.

Such differences cannot be detected in patterns (not shown) of fibers spun from higher molecular weight material of polyester **6e-5** ( $\eta_{inh} = 3.86$  dl/g), since the higher viscosity of the material prevents further orientation at higher take-up speeds.

#### 4. Conclusions

Two series of thermotropic liquid crystalline polyesters consisting of non-coplanar biphenylene units with terephthalic acid and *tert*-butyl hydroquinone (series **4**) or 6-hydroxy-2-naphthoic acid (series **6**) as comonomers have been synthesized by melt polycondensation. The stiffness of the polymer chain was varied systematically by the comonomer ratio. Most polyesters of series **4** are soluble in chloroform, whereas polyesters of series **6** are only soluble at room temperature in a mixture of trifluoro acetic acid and chloroform. In this solvent inherent viscosities up to  $\eta_{inh} = 6.57$  dl/g were determined for **4** and  $\eta_{inh} = 3.86$  dl/g for **6** by optimizing the synthetic conditions. The polyesters form nematic melts above their glass transition temperature. The nematic phase remains stable upon cooling to room temperature. Rheology measurements performed on **6e-2** ( $x = 0.6$ ) up to 30°C reveal a continuous reduction in melt viscosity by three orders of magnitude. Based on these observations these materials can be classified as nematic glasses.

Fiber spinning experiments were carried out on both types of copolyesters using a capillary melt spinner, yielding different results for series **4** and **6**. High melt viscosities prevented efficient draw-down and only modest Young's moduli in the range of 15–20 GPa were obtained for **4b** ( $x = 0.5$ ). The insufficient mechanical performance could be explained by the lack of orientation, which is also evident in SEM micrographs. As a result, the incorporation of comonomers with bulky side groups does not lead to good fiber forming materials. However, for **6e** highly oriented fibers were obtained via melt spinning at different take-up speeds. Fiber moduli between 40 and 50 GPa were attained. These show little dependence on molecular weight whereas fiber tenacity was greatly improved. WAXD patterns of the fibers confirmed the absence of crystallinity in the copolyester and improved orientation of the fibers at higher take-up speeds. In conclusion, the copolyesters with 60 mol% HNA are suitable candidates for in situ composites with PET. The results of blending experiments, fiber spinning and the evaluation of blend fiber properties as function of TLCP load level is published in the preceding contribution of this journal [35].

#### Acknowledgements

This work was partially supported by a grant from the former Hoechst-Celanese Corporation (Summit, New Jersey). The authors are indebted to Dr O.R. Hughes for helpful suggestions, support and discussions. SEM micro-

graphs were taken by C. Drummer at the BIMF, which is gratefully acknowledged.

#### References

- [1] Greiner A, Schmidt H-W. Aromatic main chain liquid crystalline polymers. In: Demus D, Goodby J, Gray GW, Spiess HW, editors. Handbook of liquid crystals, vol. 3. New York: Wiley-VCH Weinheim, 1998.
- [2] Yoon HN, Charbonneau LF, Calundann GW. Adv Mater 1992;4:206.
- [3] Han H, Bhowmik PK. Prog Polym Sci 1997;22:1431.
- [4] Schmidt H-W, Guo D. Makromol Chem 1988;189:2029.
- [5] Greiner A, Rochefort WE, Greiner K, Heffner GW, Pearson DS, Schmidt H-W. Melt and solution properties of *para*-linked aromatic LC-polyesters. In: Lemstra PJ, Kleintjens LA, editors. Integration of fundamental polymer science and technology, vol. 5. London: Elsevier Applied Science, 1991. p. 258–68.
- [6] Han H, Bhowmik PK, Frisch KC. J Polym Sci Polym Chem 1997;35:769.
- [7] Brüggling W, Kampschulte U, Schmidt H-W, Heitz W. Makromol Chem 1988;189:2755.
- [8] Schmidt H-W. Makromol Chem Makromol Symp 1989;26:47.
- [9] Choi T-G, Yun Y-K, Jin J-I. Polym Plast Technol Engng 1997;36(1):135.
- [10] Chung S-J, Huh S-M, Jin J-I. J Polym Sci A: Polym Chem 1996;34:1105.
- [11] Yun Y-K, Jin J-I, Lee MJ. J Polym Sci A: Polym Chem 1997;35:2777.
- [12] Tendolkar A, Narayan-Sarathy S, Kantor SW, Lenz RW. Polymer 1995;36:2463.
- [13] Deak DK, Lenz RW, Kantor SW. J Polym Sci A: Polym Chem 1997;35:197.
- [14] Motamedi F, Jonas U, Greiner A, Schmidt H-W. Liq Cryst 1993;14:959.
- [15] Cao MY, Varma-Nair M, Wunderlich B. Polym Adv Technol 1990;1:151.
- [16] Bi S, Zhang Y, Bu H, Luise RR, Bu JZ. J Polym Sci A: Polym Chem 1999;37:3763.
- [17] Sawyer LC, Jaffe M. J Mater Sci 1986;21:1897.
- [18] Jaffe M, Calundann G, Yoon H-N. Handbook of fiber science and technology, vol. 3. Marcel Dekker, 1989 p. 83.
- [19] Hull JB, Jones AR. Processing of liquid crystal polymers. In: Acierno D, Collyer AA, editors. Rheology and processing of liquid crystal polymers. London: Chapman and Hall, 1996. p. 86.
- [20] Savitsky AV, Gorshkova IA, Kober KJ. Makromol Sci Phys 1998;B37:119.
- [21] Bhowmik PK, Atkins EDT, Lenz RW, Han H. Macromolecules 1996;29:1910.
- [22] Joslin SL, Giesa R, Farris R. Polymer 1994;35:4303.
- [23] Giesa R, Joslin SL, Melot D, Farris RJ. Polym Polym Compos 1995;3(5):333.
- [24] Pan L, Liang BJ. Appl Polym Sci 1998;70:1035.
- [25] Radhakrishnan J, Ito H, Kikutani T, Okui N. Polym Engng Sci 1999;39:89.
- [26] Joslin SL, Jackson W, Farris. J Appl Polym Sci 1994;54:439.
- [27] Narayan-Sarathy S, Wedler W, Lenz RW, Kantor SW. Polymer 1995;36:2467.
- [28] Bruggeman A, Tinnemans AHA. J Appl Polym Sci 1999;71:1107.
- [29] Griffin BP, Cox MK. Br Polym J 1980;12:147.
- [30] Ciferri A, editor. Liquid crystallinity in polymers. New York: Weinheim VCH Publishers, 1991.
- [31] Petrovic ZS, Farris RJ. Polymer 1995;58:1349.
- [32] Ignatious F, Lu C, Kantor SW, Lenz RW. Macromolecules 1994;27:7785.
- [33] Ignatious F, Kantor SW, Lenz RW. Macromolecules 1994;27:5248.
- [34] Heitz T, Rohrbach P, Höcker H. Makromol Chem 1989;190:3295.
- [35] Grasser W, Giesa R, Schmidt H-W. Polymer, 2001;42:8517–27.

- [36] Colon I, Kelsey DR. *J Org Chem* 1986;51:2627.
- [37] Percec V, Zhao M, Bae J-Y, Hill D. *Macromolecules* 1996;29:3727.
- [38] Grasser W. PhD Thesis, University of Bayreuth, 1999.
- [39] Beery D, Kenig S, Siegmann A. *Polym Engng Sci* 1991;31:451.
- [40] Cowie JMG. *Eur Polym J* 1975;11:297.
- [41] Cogswell FN, Wissburn KF. Rheology and processing of liquid crystalline polymer melts. In: Acierno D, Collyer AA, editors. *Rheology and processing of liquid crystal polymers*. London: Chapman and Hall, 1996. p. 86.
- [42] Yoon HN. *Colloid Polym Sci* 1990;268:230.
- [43] Panar M, Avakian P, Blume RC, Gardner KH, Gierke TD, Yang HH. *J Polym Sci Polym Phys Ed* 1983;21:1955.
- [44] Thapar H, Bevis M. *J Mater Sci Lett* 1983;2:733.
- [45] Weng T, Hiltner A, Baer E. *J Mater Sci* 1986;21:744.
- [46] Savitsky AV, Gorshkova IA, Kober K. *J Macromol Sci Phys* 1998;B37:119.
- [47] Blackwell J, Biswas A. *Macromol Chem Macromol Symp* 1986;2:21.
- [48] Blackwell J, Gutierrez GA, Chivers RA. X-ray studies of thermotropic aromatic copolyesters. In: Blumstein A, editor. *Polymeric Liquid Crystals*. New York: Plenum Press, 1985. p. 167.